Influence of misch metal content on microstructure and magnetic properties of R–Fe–B magnets sintered by dual alloy method*

Rong-Xiang Shang(商荣翔)[1,2], Jie-Fu Xiong(熊杰夫)[1,2], Dan Liu(刘丹)[1,2], Shu-Lan Zuo(左淑兰)[1,2], Xin Zhao(赵鑫)[1,2], Rui Li(李锐)[1,2], Wen-Liang Zuo(左文亮)[1,2], Tong-Yun Zhao(赵同云)[1,2], Ren-Jie Chen(陈仁杰)[2,3], Ji-Rong Sun(孙继荣)[1,2], and Bao-Gen Shen(沈保根)[1,2,†]

[1] *State Key Laboratory of Magnetism, Institute of Physics, Chinese Academy of Sciences, Beijing* 100190, *China*
[2] *University of Chinese Academy of Sciences, Beijing* 100049, *China*
[3] *Key Laboratory of Magnetic Materials and Devices, Ningbo Institute of Materials Technology and Engineering, Chinese Academy of Sciences, Ningbo* 315201, *China*

(Received 20 February 2017; revised manuscript received 7 March 2017; published online 30 March 2017)

$MM_{14}Fe_{79.9}B_{6.1}$/$Nd_{13.5}Fe_{80.5}B_6$ magnets were fabricated by dual alloy method (MM, misch metal). Some magnets have two Curie temperatures. Curie temperatures T_{c1} corresponds to the main phase which contains more LaCe, and T_{c1} decreases from 276.5 °C to 256.6 °C with the content of MM increasing from 30.3 at.% to 50.6 at.%. The variation of B_r with the increase of MM indicates the existence of inter-grain exchange coupling in the magnets. When MM/$R \leq 30.3$ at.%, the magnetic properties can reach the level of the intrinsic coercivity $H_{cj} \geq 7.11$ kOe and the maximum energy product $(BH)_{max} \geq 41$ MGOe. Compared with Nd, La and Ce are easier to diffuse to the grain boundaries in the sintering process, and this will cause the decrease of H_{cj}. Due to the diffusion between the grains, the atomic ratio of La, Ce, Pr, and Nd in each grain is different and the percentage of Nd in all grains is higher than that in misch metal.

Keywords: misch metal, multiple-main-phase, grain, permanent magnet

PACS: 75.50.Vv, 75.50.Ww **DOI:** 10.1088/1674-1056/26/5/057502

1. Introduction

Since Nd–Fe–B magnets were invented in 1983,[1] they are widely used in many fields due to their high magnetic performance, such as hybrid electric vehicles (HEV), wind turbines, voice-coil motor (VCM) devices, magnetic resonance imaging (MRI), etc.[2–5] In light rare earth, not only the abundance of Nd is less than La and Ce but also its price is much higher,[6] but the magnetic performances of La–Fe–B and Ce–Fe–B are much lower than Nd–Fe–B.[7] Therefore, the substitution of La, Ce for Nd in Nd–Fe–B to find a balance between magnetic performance and cost is an important research domain.[8–10] Okada *et al.*[11] studied $(Ce_{0.4}Pr_{0.1}Nd_{0.5})_{32.5-34.5}Fe_{bal}B_{1-1.6}$ sintered magnets, and obtained the best magnetic propertied as $(BH)_{max} = 27$ MGOe and $H_{cj} = 5.3$ kOe. Zhu *et al.*[12] reported the remarkable values of $(BH)_{max} = 43.3$ MGOe and $H_{cj} = 9.26$ kOe for sintered $(Nd_{0.7}Ce_{0.3})_{30}(Fe,TM)_{bal}B_1$ magnet. For nanocrystalline magnets, Tang *et al.*[13] obtained $(BH)_{max} = 18.99$ MGOe and $H_{cj} = 3.6$ kOe in $[(La_{0.35}Ce_{0.65})_{0.4}Nd_{0.6})]_{15.5}Fe_{77}B_{7.5}$ magnet. Misch metal (MM, typically consisting of 28.0 at.% La, 52.0 at.% Ce, 5.1 at.% Pr, 14.7 at.% Nd, 0.2 at.% others) is an intermediate product in rare earth extraction process, and it does not need the separation of La, Ce, Pr, and Nd elements, which reduces the cost.[14] In the work by Ko *et al.*,[15] $(BH)_{max} = 7.6$ GOe and $H_{cj} = 5.81$ kOe were achieved by melt-spun $MM_{12.5}Fe_{78.9}B_{8.6}$ alloy. Zhang *et al.*[16] found $(BH)_{max} = 10.14$ MGOe and $H_{cj} = 6.29$ kOe for melt-spun $MM_{2.4}Fe_{14}B$ ribbon. There are few reports on sintered MM–Fe–B. Zhu *et al.*[12] deemed that the dual-main-phase alloy method can realize the adjustment of the composition and combination of main phases of the magnets and there is almost no decrease in remanence. Moreover, the increasing discrepancy of the magnetocrystalline fields between the dual main phases will enhance the coercivity of the magnets. Based on the above studies, in this work, the double main phase alloy method was used to fabricate different ratios of $MM_{14}Fe_{79.9}B_{6.1}$/$Nd_{13.5}Fe_{80.5}B_6$ magnets. The magnetic properties, Curie temperature, and change of elements in the grains have been studied in detail.

2. Experiment

An alloy with near-stoichiometric composition of $MM_{14}Fe_{79.9}B_{6.1}$ (at.%) was prepared by induction melting and subsequent strip-casting (SC). Though hydrogen decrepitating (HD) and jet-milling (JM), approximately 3.0 μm powders were prepared. The powders of $MM_{14}Fe_{79.9}B_{6.1}$ were defined as M. Powders of $Nd_{13.5}Fe_{80.5}B_6$ were prepared by the same way and defined as N. Then M and N were mixed evenly according to the proportion of M: 0 wt.%, 10 wt.%, 30 wt.%, 40 wt.%, 50 wt.%, 100 wt.%, respectively. Then the mixed

*Project supported by the National Key Research and Development Program of China (Grant Nos. 2014CB643702 and 2016YFB0700903), the National Natural Science Foundation of China (Grant No. 51590880), and the Knowledge Innovation Project of the Chinese Academy of Sciences (Grant No. KJZD-EW-M05).

†Corresponding author. E-mail: shenbg@aphy.iphy.ac.cn

© 2017 Chinese Physical Society and IOP Publishing Ltd

powders were aligned and compacted under a magnetic field of 1.8 T and a pressure of $\sim$ 5 MPa in an N_2-filled glove box, followed by an isostatic pressing at $\sim$ 160 MPa. The green compacts were sintered at 1040 °C for 2 h, followed by a two-step tempering treatment, which was performed at 900 °C for 2 h and at 520 °C for 2 h, respectively. The atomic ratios of LaCe/*R* and the atomic compositions of the samples are shown in Table 1 (*R* represents the total rare earth).

The density of the magnets was measured based on Archimedes principle. The Curie temperature was measured by Model 4 HF-VSM. The phase component of the magnets were characterized by x-ray diffraction (XRD) using a Rigaku D/Max-2400 diffractometer with Cu $K\alpha$ radiation. The magnetic properties of the magnets, including the remanence (B_r), the intrinsic coercivity (H_{cj}), and the maximum energy product ($(BH)_{max}$), were measured by quasi-closed loop permanent magnetic measurement system NIM-500C. The microstructure of the magnets was examined and characterized by a XL30 S-FEG scanning electron microscope (SEM) equipped with an energy dispersive x-ray spectroscopy (EDS).

Table 1. Compositions of different samples.

Sample	(M/(M+N))/wt.%	(MM/*R*)/at.%	(LaCe/*R*)/at.%	Atomic composition
M_0	0	0	0	$Nd_{13.5}Fe_{80.5}B_6$
M_{10}	10	10.3	8.2	$La_{0.39}Ce_{0.73}Pr_{0.07}Nd_{12.35}Fe_{80.44}B_{6.01}$
M_{30}	30	30.3	24.3	$La_{1.18}Ce_{2.18}Pr_{0.21}Nd_{10.08}Fe_{80.32}B_{6.03}$
M_{40}	40	40.5	32.4	$La_{1.57}Ce_{2.91}Pr_{0.28}Nd_{8.94}Fe_{80.26}B_{6.04}$
M_{50}	50	50.6	40.5	$La_{1.96}Ce_{3.64}Pr_{0.35}Nd_{7.8}Fe_{80.2}B_{6.05}$
M_{100}	100	100	80.2	$La_{3.92}Ce_{7.28}Pr_{0.7}Nd_{2.1}Fe_{79.9}B_{6.1}$

3. Results and discussion

Figure 1 shows XRD patterns of the surface perpendicular to the alignment direction of the magnets with different compositions. From the pattern, it is not obvious that the magnets are composed of two main phases. Meanwhile, the intensities and 2θ values of the diffraction peaks have no change with the increase of the MM content. That is because the lattice constants of $La_2Fe_{14}B$, $Ce_2Fe_{14}B$, $Pr_2Fe_{14}B$, and $Nd_2Fe_{14}B$ are very close to each other.[7] It is hard to distinguish them from XRD patterns.

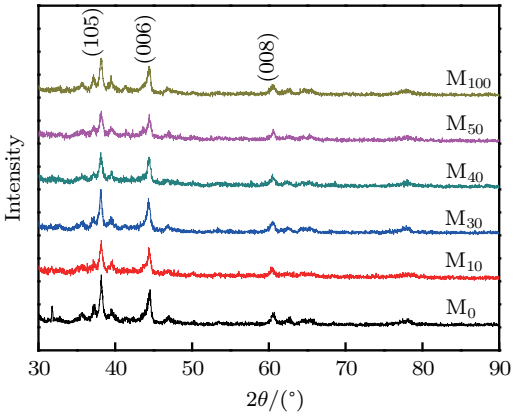


Fig. 1. (color online) XRD patterns of the magnets with different compositions.

In order to ascertain whether the sintered magnets are composed of two main phases or not, the magnetization dependence on temperature of the sintered magnets was measured at the magnetic field of 500 Oe. The curves of the magnetization and dM/dT are shown in Fig. 2. It can be seen that the curves of dM/dT for M_{30}, M_{40}, and M_{50} magnets have two peaks, which correspond to the two Curie temperatures. In order to facilitate the following discussion, the lower Curie temperature is defined as T_{c1} and the higher one is defined as T_{c2}, and they are summarized in Table 2. It also can be seen that M_{10} magnet has only one peak, which may be due to the lack of $MM_{14}Fe_{79.9}B_{6.1}$ and $MM_{14}Fe_{79.9}B_{6.1}$ diffused seriously in the sintering process. T_{c1} is not a constant and decreases from 276.5 °C to 256.6 °C with the content of $MM_{14}Fe_{79.9}B_{6.1}$ increasing from 30 wt.% to 50 wt.%. That is mainly because that M_{30}, M_{40}, and M_{50} magnets are not dual main phase but multiple main phase. Specifically, in the sintering process, the rare earth atoms of $MM_{14}Fe_{79.9}B_{6.1}$ and $Nd_{13.5}Fe_{80.5}B_6$ ineluctably diffused to each other, the atomic ratio of La, Ce, Pr, and Nd in the grains was not the same to others. Finally, the ratio formed a continuous distribution and this result is shown in Table 3. T_{c1} corresponds to the main phase which contains more LaCe, and T_{c2} corresponds to the main phase which contains more PrNd. The Curie temperatures of $La_2Fe_{14}B$ and $Ce_2Fe_{14}B$ are 257 °C and 157 °C, respectively.[7] Therefore, with the increase of LaCe in the main phase, T_{c1} decreases. T_{c2} is 296.6 °C and almost does not change when the content of $MM_{14}Fe_{79.9}B_{6.1}$ increases from 10 wt.% to 50 wt.%. The reason for this may be that Nd diffuses more readily into the grains of $MM_2Fe_{14}B$ compared to La and Ce into $Nd_2Fe_{14}B$ at the sintering temperature of 1040 °C. It is generally known that La–Fe–B is hard to form 2:14:1 phase and Ce–Fe–B to form 2:14:1 phase needs a lower sintering temperature.[17,18]

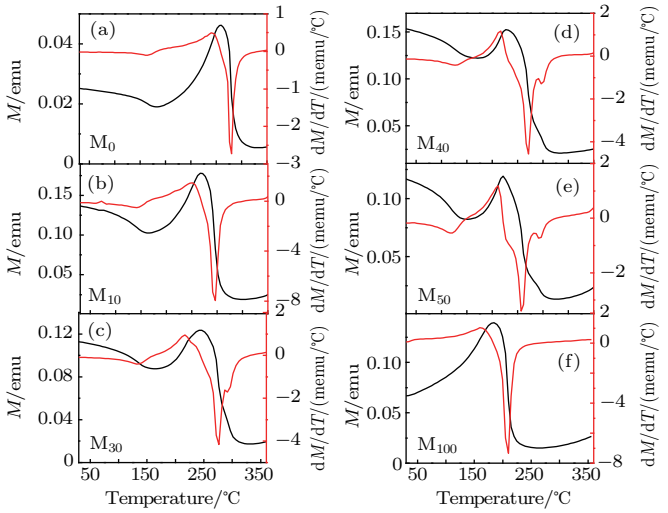


Fig. 2. (color online) Temperature dependence of magnetization and dM/dT of the sintered magnets: (a) M_0, (b) M_{10}, (c) M_{30}, (d) M_{40}, (e) M_{50}, (f) M_{100}.

Table 2. Curie temperatures of the sintered magnets.

Sample	T_{c1}/°C	T_{c2}/°C
M_0	–	326.4
M_{10}	–	296.6
M_{30}	276.5	296.6
M_{40}	271.6	296.6
M_{50}	256.6	296.6
M_{100}	210	–

The magnetic properties of the magnets and their variations as functions of MM/R are shown in Fig. 3. The densities of the magnets are about 7.53 g/cm^3 and almost do not change with the increase of MM content in Fig. 3(a). It means that the magnets are completely densified at the sintering temperature of 1040 °C. The values of B_r, H_{cj}, and $(BH)_{max}$ for the magnets decrease drastically with the increase of MM content. The J_s for $La_2Fe_{14}B$ and $Ce_2Fe_{14}B$ are 1.38 T and 1.17 T, respectively,[7] which are lower than those of $Nd_2Fe_{14}B$ and $Pr_2Fe_{14}B$. That is why B_r decreases with increasing MM content. The B_r for $Nd_{13.5}Fe_{80.5}B_6$ and $MM_{14}Fe_{79.9}B_{6.1}$ are 13.79 kGs and 10.28 kGs, respectively, and are connected by a red line. It can be clearly seen that the values of B_r for the multiple-main-phase magnets are all above the red line, indicating that there exists inter-grain exchange coupling in the sintered magnets.[19] In Figs. 3(c) and 3(d), H_{cj} decreases from 11.96 kOe to 0.65 kOe, meanwhile, $(BH)_{max}$ decreases from 47.38 MGOe to 2.72 MGOe with the MM content increasing from 0 at.% to 100 at.%.

The decline of H_{cj} is due to the lower intrinsic magnetocrystalline anisotropy field of $La_2Fe_{14}B$ and $Ce_2Fe_{14}B$ than that of $Nd_2Fe_{14}B$.[7] The values of H_{cj} for the multiple-main-phase magnets are all under the red line, this can be attributed to the changes of microstructure and phase component. Compared with Nd, La and Ce are easier to diffuse to grain boundaries in the sintering process, and they will cause deterioration of grain boundaries.[13,20] The values of $(BH)_{max}$ for the multiple-main-phase magnets are all above the red line, this is due to the changes of B_r. When MM/$R \leq 30.3$ at.%, the magnetic properties can reach the level of $B_r \geq 13.12$ kGs, $H_{cj} \geq 7.11$ kOe, and $(BH)_{max} \geq 41$ MGOe. The $(BH)_{max}$ and H_{cj} are larger than 34 MGOe and 4.84 kOe, respectively, when MM/R is up to 50 at.%. If a small quantity of elements, such as Al or Cu, are added to the magnets, the H_{cj} will get a further increase.[21] These magnets can be applied in the field where high coercivity is not required, and also have a cost advantage.

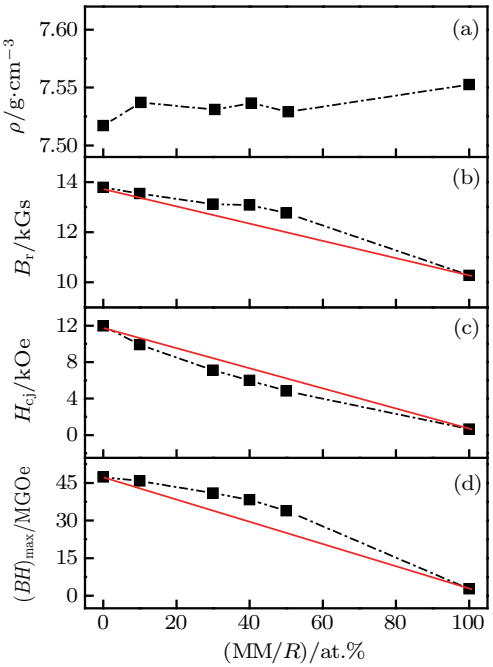


Fig. 3. (color online) Dependence of density and magnetic properties on MM/R of the sintered magnets (red line connects corresponding points of MM/R = 0 and MM/R = 100).

Back-scattered electron images of the polished magnets after two stage tempering are shown in Fig. 4. There are no obviously continuous grain boundaries between main phase grains, and a great quantity of grains merge each other. This will enhance the exchange coupling between them and lead to the increase of B_r and the decrease of H_{cj}. Most grain sizes are less than 10 μm, and evenly distributed. It also can be seen that it is very hard to distinguish different grains in the M_{100} magnet compared with others because of the serious diffusion of La and Ce. This has been discussed in our previous work.[22] Due to the diffusion between the grains, the atomic ratio of La, Ce, Pr, and Nd in each grain is different. The percentages of La, Ce, Pr, and Nd of ten grains which are randomly selected from the M_{40} magnet are analyzed by EDS. In order to facilitate observation, the results are listed in Table 3 according to the percentage of Nd. With the increase of Nd, the percentages of La and Ce decrease. The percentage of Nd in all grains is greater than that in misch metal (14.7 at.%), which indicates that La and Ce diffuse more easily than Nd. The percentages of La, Ce, Pr, and Nd in some grains are very close to

each other, such as 5# and 6#. It may be due to that their surroundings are very close. Therefore, it can be concluded that the M_{40} magnet is not dual-main-phase magnet but multiple-main-phase magnet. The magnets M_{10}, M_{30}, M_{50}, and M_{100} are also multiple-main-phase magnets.

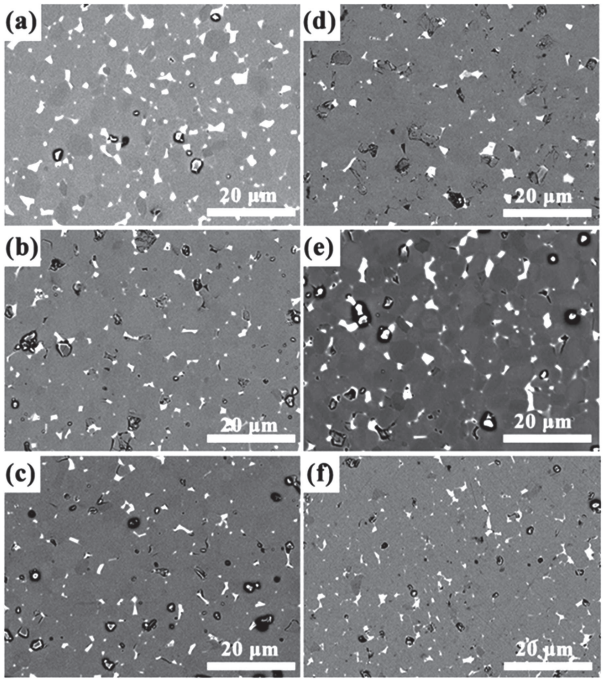


Fig. 4. SEM-back scattered micrographs of the sintered magnets: (a) M_0, (b) M_{10}, (c) M_{30}, (d) M_{40}, (e) M_{50}, (f) M_{100}.

Table 3. ESD analysis of the percentages of La, Ce, Pr, and Nd in the grains of the M_{40} magnet.

Number	Nd	Ce	La	Pr
1#	23.71	49.48	23.71	3.09
2#	52.08	32.29	13.54	2.08
3#	60.19	25.93	12.04	1.85
4#	72.95	16.39	9.02	1.64
5#	82.61	11.30	6.09	0.00
6#	83.05	10.17	5.93	0.85
7#	86.24	10.09	3.67	0.00
8#	87.62	8.57	2.86	0.95
9#	95.37	2.78	1.85	0.00
10#	96.15	1.92	1.92	0.00

4. Conclusion

$MM_{14}Fe_{79.9}B_{6.1}/Nd_{13.5}Fe_{80.5}B_6$ multiple-main-phase magnets of different ratios were fabricated by conventional sintering method. It is hard to distinguish them from XRD patterns. For the dM/dT curves derived from the magnetization dependence on temperature, M_{10} magnet has only one peak, which may be due to that $MM_{14}Fe_{79.9}B_{6.1}$ diffused seriously in the sintering process. T_{c1} decreases from 276.5 °C to 256.6 °C with the content of $MM_{14}Fe_{79.9}B_{6.1}$ increasing from 30 wt.% to 50 wt.%. But T_{c2} is 296.6 °C and almost has no change. The densities of the magnets are about 7.53 g/cm^3 and completely densified. The B_r, H_{cj}, and $(BH)_{max}$ of the magnets decrease drastically with the increase of MM content. When MM/$R \leq 30.3$ at.%, the magnetic properties can reach the level of $H_{cj} \geq 7.11$ kOe and $(BH)_{max} \geq 41$ MGOe. The atomic ratio of La, Ce, Pr, and Nd in each grain is different and the percentage of Nd in all grains is greater than that in misch metal. The magnets M_{10}, M_{30}, M_{40}, M_{50}, and M_{100} are not dual-main-phase magnets but are multiple-main-phase magnets.

References

[1] Sagawa M, Fujimura S, Togawa N and Matsuura Y 1984 *J. Appl. Phys.* **55** 2083
[2] Jiles D C 2003 *Acta Mater.* **51** 5907
[3] Yu X Q, Yue M, Liu W Q, Li Z, Zhu, M G and Dong S Z 2016 *J. Rare Earth* **34** 614
[4] Liu W Q, Yue M, Cui B Z and Hadjipanayis G C. 2014 *Rev. Nanosci. Nanotechnol.* **3** 259
[5] Yue M, Li Y Q, Wu Q and Liu W Q 2014 *Rev. Nanosci. Nanotechnol.* **3** 276
[6] Pei K, Zhang X, Lin M and Yan A R 2016 *J. Magn. Magn. Mater.* **398** 96
[7] Burzo E 1998 *Rep. Prog. Phys.* **61** 1099
[8] Xing M Y, Han J Z, Lin Z, Wan F M, Li C, Liu S Q, Wang C S, Yang J B and Yang Y C 2013 *J. Magn. Magn. Mater.* **331** 140
[9] Chang W C, Wu S H, Ma B M and Bounds C O 1997 *J. Magn. Magn. Mater.* **167** 65
[10] Wang X C, Zhu M G, Li W, Zheng L Y, Zhao D L, Du X and Du A 2015 *Electron. Mater. Lett.* **11** 109
[11] Okada M, Sugimoto S, Ishizaka C, Tanaka T and Homma M 1985 *J. Appl. Phys.* **57** 4146
[12] Zhu M G, Li Wei, Wang J D, Zheng L Y, Li Y F, Zhang K, Feng H B and Liu Tao 2014 *IEEE Trans. Magn.* **50** 1000104
[13] Tang W Z, Zhou S Z and Wang R 1989 *J. Appl. Phys.* **65** 3142
[14] Niu E, Chen Z A, Chen G A, Zhao Y G, Zhang J R, Hu X L, Wang B P and Zhen X 2014 *J. Appl. Phys.* **115** 113912
[15] Ko Y K, Yoon S and Booth J G 1997 *J. Magn. Magn. Mater.* **176** 313
[16] Zhang M, Shen B G, Hu F X and Sun J R 2015 *IEEE Trans. Magn.* **51** 2103304
[17] Zhang X F, Shi Y, Ma Q, Liu Y L, Shi M F, Li Y F, Wang G F and Zhao Z R 2015 *Rare Metal Mat. Eng.* **44** 748
[18] Yan C J, Guo S, Chen R J, Lee D and Yan A R 2014 *IEEE Trans. Magn.* **50** 2104604
[19] Hussain M, Zhao L Z, Zhang C, Jiao D L, Zhong X C and Liu Z W 2016 *Physica B* **483** 69
[20] Pathak A K, Khan M, Jr K A G, McCallum R. W, Zhou L, Sun K W, Dennis K W, Zhou C, Pinkerton F. E, Kramer M J and Pecharsky V K 2015 *Adv. Mater.* **27** 2663
[21] Pandian S, Chandrasekaran V, Markandeyulu G, Iyer K J L and Rama Rao K V S 2002 *J. Appl. Phys.* **92** 6082
[22] Shang R X, Xiong J F, Li R, Zuo W L, Zhang J, Zhao T Y, Chen R J, Sun J R and Shen B G 2017 *AIP Adv.* **7** 056215